Passive and active optical fibers for space and terrestrial applications

Mansoor Alam*, Jaroslaw Abramczyk, Julia Farroni, Upendra Manyam, Douglas Guertin
Nufern, 7 Airport Park Road, East Granby, CT 06026

ABSTRACT

Being the new frontier of science and technology, as the near earth space begins to attract attention, low cost and rapidly deployable earth observation satellites are becoming more important. Among other things these satellites are expected to carry out missions in the general areas of science and technology, remote sensing, national defense and telecommunications. Except for critical missions, constraints of time and money practically mandate the use of commercial-off-the-shelf (COTS) components as the only viable option. The near earth space environment (~50-50000 miles) is relatively hostile and among other things components/devices/systems are exposed to ionizing radiation. Photonic devices/systems are and will continue to be an integral part of satellites and their payloads. The ability of such devices/systems to withstand ionizing radiation is of extreme importance. Qualification of such devices/systems is time consuming and very expensive. As a result, manufacturers of satellites and their payloads have started to ask for radiation performance data on components from the individual vendors. As an independent manufacturer of both passive and active specialty silica optical fibers, Nufern is beginning to address this issue. Over the years, Nufern has developed fiber designs, compositions and processes to make radiation hard fibers. Radiation performance data (both gamma and proton) of a variety of singlemode (SM), multimode (MM), polarization maintaining (PM) and rare-earth doped (RED) fibers that find applications in space environment are presented.

Keywords: Gamma radiation, Proton radiation, Induced attenuation, Attenuation recovery, Dose rate, Total dose, SM fiber, MM fiber, PM fiber, EDF.

1. INTRODUCTION

Near earth orbiting satellites (low, middle, geostationary, etc.) carry out missions in the general areas of earth and space science, technology demonstration, remote sensing, commercial telecommunication and national defense. Two examples of satellite missions from each market segment are presented in Table 1. Satellites carrying out remote sensing and military missions usually operate in the low earth orbits (LEO) at altitudes of 300-600 miles and 600-1200 miles, respectively, [1] whereas satellites intended for science and technology missions operate in the middle earth orbits (MEO) at altitudes of 3000-12000 miles.[1] Telecommunication satellites however, operate in geostationary orbits (GEO) at much higher altitudes of 23000-50000 miles.[1] The mission of the satellite dictates the choice of the orbital path which may take it through the South Atlantic Anomaly (LEO), Van Allen radiation belts[2] (MEO) and cosmic rays (GEO). The South Atlantic Anomaly exists at altitudes of 250-750 miles (depending on the latitude) and is dominated by energetic protons (> 10 MeV). The outer Van Allen radiation belt begins at 6200 miles (depending on latitude) and extends to altitudes of 37000-57000 miles. It is dominated by energetic electrons (1-10 MeV). Interiors of the satellites are therefore shielded to some extent to minimize radiation exposure of the payload.

Table 1. Sampling of satellite missions (past and present).

Market Segment	Satellite
Earth and Space Science	Geoscience Laser Altimeter System (GLAS), Solar Radiation and Climate Experiment (SORCE)
Technology Demonstration	Earth Observing-1 (EO-1), Proba-2
Remote Sensing	Lightning Patterns and Weather System (OrbView-1), Weather Prediction, Climate and Gravity Research (FORMSAT)
Telecommunications	Direct Broadcast Satellites (EchoStar i-x), Global Data Communication (MicroStar)
National Defense	Electronic Intelligence (Cosmos-2406), Radar Intelligence (Hercules)

*malam@nufern.com; Ph: (860) 408-5000; Fax: (860) 408-5080; www.nufern.com

All the aforementioned applications rely heavily on the use of onboard photonic devices and systems. Silica optical fibers are used in fiber lasers, fiber amplifiers, fiber sensors, etc. They are also used in onboard data processing, communication and transmission equipments, and as communication links between various devices. The extensive use of silica optical fibers in LEO satellites is a source of concern because of the radiation environment in which these satellites operate and the uncertainty about the reliability of components, devices and systems based on silica optical fibers in such environments. Although the performance will depend on the actual mission radiation environment, it is safe to assume that the average radiation dose rate received by the shielded interior of a typical satellite is ~0.04 Rad/min.[3] For a 1-5 year mission lifetime, this translates to a total accumulated dose of ~20-105 kRad, which may be sufficient to degrade the performance of the spacecraft's optical components.

When an optical fiber is exposed to ionizing radiation, it "optically" darkens. This happens because the chemical bonds in the core and the cladding materials are disrupted, resulting in the appearance of new electronic transition states giving rise to additional absorption in the wavelength region of interest. Once the radiation source is removed, the fiber returns to its original state (a process called recovery). Almost all fibers experience some degree of permanent damage (partial recovery) which is a source of concern. If the dose rate is low, an equilibrium state (between attenuation and recovery) is reached with some degree of darkening. If the dose rate is high, the utility of the fiber depends on the overall induced attenuation and the recovery time. The attenuation depends on the core/cladding glass composition, while the recovery time depends on the temperature. Since attenuation is composition dependent, fibers having pure silica cores and fluorine down doped claddings are amongst the most radiation hard fibers. Presence of dopants in the core and/or cladding such as germanium, phosphorus and boron increase the radiation induced attenuation of the fiber relative to pure silica and are therefore not desirable in fibers destined for use in space.[4] There is evidence to suggest that fluorine doping decreases the radiation induced attenuation particularly at the lower wavelengths.[5] Rare earth elements such as erbium, ytterbium, neodymium and thulium that are essential ingredients of active silica optical fibers are also not desirable in fibers to be used in space applications because the pump and the signal absorption behaviors of these active fibers is significantly modified by the space radiation environment. Metallic entities like aluminum (which is commonly present in the active fibers) make these fibers extremely sensitive in radiation environments.

The behavior of silica optical fiber in a radiation environment also depends on how the fiber is manufactured, and as such the radiation performance of the same fiber may vary from vendor to vendor. The conditions under which the silica glass is deposited lead to generation of intrinsic defects in the silica glass network, causing enhanced radiation induced attenuation. Similarly, the conditions under which the glass is drawn lead to the formation of defects that become active upon radiation exposure, giving rise to higher than normal attenuation. It is necessary to carefully manipulate and control the process parameters; this may be simpler with some processes and difficult in other cases.

The coating that is applied to silica optical fibers, particularly the primary coating, also plays an important role in how the fiber will perform in a radiation environment. Thermally cured polyimide coated fibers perform better than UV cured acrylate coated fibers from the point of view of radiation induced attenuation. Most likely, it is both the coating material itself and the coating application temperature that control radiation induced attenuation. In a radiation environment, the low index fluoro-acrylate coatings that are normally applied to active fibers of the double clad design experience more damage than regular UV cured acrylate coatings.

Radiation induced attenuation of silica optical fibers also depends very strongly on the radiation dose rate and test conditions. The induced loss increases with increasing dose rate. During measurements, it is beneficial to keep the dose rates small in order to mimic the space radiation environment. Measurement temperature also plays an important role. Radiation induced attenuation decreases with increasing exposure temperature due to faster recovery kinetics. Lower temperature measurements therefore provide the "worse case" scenario. Measurements at lower wavelengths reveal much higher radiation induced attenuation in comparison to measurements at higher wavelengths.

Significant amounts of work have been carried out to characterize the performance of optical fibers in various radiation environments. Qualifying the fibers for use in space is time consuming and expensive. The situation is further aggravated by the fact that some vendors of such optical fibers have ceased to exist or have shifted priorities, resulting in a scarcity of such fibers and radiation data. Many of the fibers qualified in the past are no longer available.

Except for critical missions, constraints of time and money practically mandate the use of COTS components as the

Table 2. Typical radiation tolerances of COTS and radiation hard components.

Parameter	COTS	Radiation Hard
Total Accumulated Dose (Rads)	10^3 - 10^4	10^5 - 10^6
Dose Rate Upset (Rads/s)	10^6 – 10^8	10^9 – 10^{10}
Dose Rate Induced Latchup (Rads/s)	10^7 – 10^9	10^{12} – 10^{14}
Single Event Upset (Errors/bit-day)	10^{-3} - 10^{-7}	10^{-8} - 10^{-10}

only viable option. Typical radiation tolerances of COTS and radiation hard components are presented in Table 2. Manufacturers of satellites and their payloads have already started to demand radiation performance data on components from the individual component vendors. As an independent manufacturer of both passive and active specialty optical fibers, Nufern is beginning to address this issue. Over the years, Nufern has developed fiber designs, compositions and processes to make radiation hard fibers. Radiation performance data (both gamma and proton) of a variety of singlemode, multimode, polarization maintaining and rare-earth doped fibers that find applications in space environments, are presented.

2. EXPERIMENTAL

2.1 Tested Fibers

The Nufern fibers that were tested for resistance against gamma and proton radiation induced attenuation are listed in Table 3. Details on the specifications of these fibers can be found on Nufern's website.[6] Two reference fibers were also tested. These were Corning's SMF28® and Sumitomo's Z-fiber®.[7-8]

2.2 Gamma Radiation Testing

The gamma radiation facility used for testing was an irradiation room having a volume of 14.5 m^3. A wide range of dose rates (100 Rad/hr - 1 MRad/hr) from a Co^{60} source were available. Several small ports penetrated one shielding wall to provide access for instrumentation cables. Test fiber was wound on a 150-mm diameter spool which was mounted on a shaft that rotated it back-and-forth on its central axis by 360° at a rate of ~0.6 rpm in order to directly expose the entire length of fiber to gamma radiation. Dosimetry mapping was performed to determine the uniformity of the gamma radiation dose rate over the spool. Bruker Biopsin Alanine pellets were used as dosimeters. Average dose rate used was ~2 Rad/sec and data was accumulated to a total dose of 50 kRad. All measurements were carried out at room temperature.

An OTDR (PK Model 6500) was used for loss measurements of all the fibers except PM850G-80. The fiber under measurement was spliced to a lead fiber (SMF28®) spool to extend the length of the signal, thereby improving measurement accuracy. Radiation induced attenuation of PM850G-80 fiber at 830 nm was measured using a Qphotonics SLED source (820 nm), Agilent Model 81624A InGaAs detector and an Agilent Lightwave multimeter Model 8160A with 81619A interface. Input power was below 1 µW (30 dBm) to avoid photobleaching effects.

2.3 Proton Radiation Testing

Table 3. Tested fibers.

γ-Radiation	Proton Radiation
S1550-HTA (SM)	S1550-HTA (SM)
R1310-HTA (SM)	PM1300G-80 (SM)
GR50/125-23-HTA (MM)	EDFL-980-HP (RED)
GR62.5/125-27-HTA (MM)	Corning SMF28® (SM)
GR100/140-24-HTA (MM)	Sumitomo Z-fiber® (SM)
PM1550G-80 (SM)	
PM850G-80 (SM)	
Corning SMF28® (SM)	

Measurements were also carried out in a proton accelerator facility. The proton beam diameter over which the energy was uniform was 100 mm. Several small ports penetrated one shielding wall to provide access for instrumentation cables. Fibers were wound on a custom Plexiglas® spool of a "wedding cake" design. This allowed simultaneous exposure of up to seven fibers without energy loss due to shadowing, with separate data acquisition parameters for each fiber. The spool was precisely aligned with a laser that was coaxial with the proton beam.

Transmission of the fibers was monitored simultaneously and continuously during and for several hours after the end of exposure. For S1550-HTA and Z-fiber® data was collected at 1570 nm, while for PM1300G-80 and SMF28® data was collected at 1310 nm. For EDFL-980-HP, LEDs were centered at 980 nm, 1300 nm and 1510 nm. Protons had energy of 55 MeV, flux was ~1.1×10^{8} protons/cm^2-s corresponding to a gamma dose rate of ~33 Rad/sec, and fluence was ~1.47×10^{12}/cm^2 corresponding to ~500 kRad. During and after the irradiation, temperature was held at ~27°C.

3. RESULTS AND DISCUSSION

3.1 Gamma Radiation Testing of SM Fibers

S1550-HTA is a SM pure silica core (PSC) fiber containing fluorine down-doped cladding and is considered as a "radiation hard" fiber. It finds applications in optical fiber sensors where the fiber is likely to be exposed to extremely high dose rates and total doses. R1310-HTA is also a SM fiber that is optically and mechanically similar to SMF28® but is manufactured in a manner to impart higher radiation resistance in comparison to SMF28®. It is considered as a "radiation tolerant" fiber and is designed to replace SMF28® in applications where ionizing radiation is of concern.

Induced attenuation versus accumulated dose plots of S1550-HTA, R1310-HTA and SMF28® fibers at 1550 nm are presented in Fig. 1. Solid lines represent best-fit to the data. In case of S1550-HTA, data is well represented by a three-term "saturating exponentials " model:[9]

$$A = \sum_i a_i[1-\exp(-D/\tau_i)] \tag{1}$$

where A is the induced attenuation, D is the accumulated dose, and a_i and τ_i are the best fit parameters describing the amplitude and the saturating dose, respectively of the different exponentials. Each term represents an absorbing defect. In case of R1310-HTA and SMF28®, data is well represented by a much simpler "power law" model:[10]

$$A = \alpha D^{\beta} \tag{2}$$

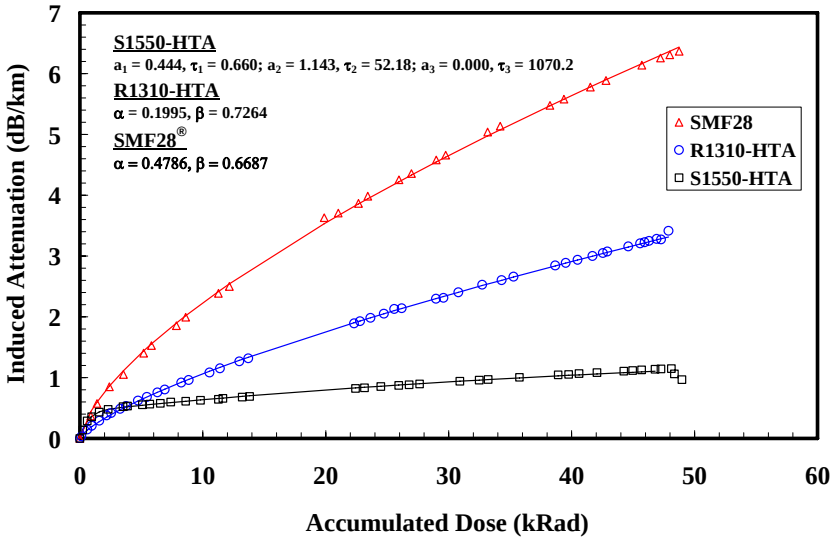

Fig. 1. γ-radiation data of the single mode fibers at 1550 nm.

where α and β are the best fit parameters describing the power function. Best fit constants of all the three fibers are listed in Fig. 1 and can be used to predict induced attenuation at any given accumulated dose.

First, the radiation data of SMF28® acquired in this study is compared with the data available in published literature.[11] It is difficult to make such a comparison because of the differences in dose rates, total doses, and testing temperatures. However, if data is available at two dose rates, it is possible to extract radiation induced attenuation at any given dose rate and total dose. The dose rate dependent constant α in Eq. 2 is described by the following equation:[12]

$$\alpha = \alpha_o [\phi]^{(1-\beta)/n} \tag{3}$$

where α_o is the dose rate independent constant, ϕ is the dose rate and n is the kinetic order of recovery (usually 1 or 2). If a value of n is assumed and a minimum of two sets of data (ϕ_1, D_1, A_1) and (ϕ_2, D_2, A_2) are available, then it is possible to determine the values of α_o and β for predicting A at any value of ϕ and D. A comparison is shown in Table 4. Actual data is presented in regular style while the extrapolated data (under conditions similar to those used by Nufern) using the method described above is shown in italics along with the data collected by Nufern. Attenuation measured in this study is somewhat higher than the attenuation extracted from data reported in the literature.[11]

According to Fig. 1, under similar irradiation conditions, S1550-HTA fiber is superior to both R1310-HTA and SMF28®. At a dose rate of ~2.13 Rad/sec, attenuation of S1550-HTA fiber increases rapidly to ~0.5 dB/km at a total dose of ~2.25 kRad where it reaches saturation. From there on, attenuation increases slowly till it reaches ~1.1 dB/km at ~50 kRad. At lower dose rate exposures, this fiber will certainly reach saturation at much lower total doses. The only meaningful comparison can be made with Sumitomo's Z-fiber® (SM, pure silica core fiber) that is considered as a high radiation hardness fiber. The gamma radiation induced attenuation of this fiber at room temperature is ~1.5 dB/km when tested at a dose rate of 27.8 Rad/sec and after a total accumulated dose of 100 kRad.[8] At the same accumulated dose, but at an order of magnitude lower dose rate, induced attenuation of S1550-HTA fiber is predicted to be 1.4 dB/km (by using Eq. 1 and the data in Fig. 1). This estimation assumes that the data can be extrapolated from 50 kRad to 100 kRad.

With respect to R1310-HTA fiber, data in Fig. 1 clearly indicates the superior radiation hardness of Nufern fiber as opposed to that of SMF28® under similar irradiation conditions. There is at least one fiber manufactured by J- Fiber which is optically similar to SMF28® and is marketed as radiation resistant SM fiber.[13] Gamma radiation induced attenuation of this fiber at 1550 nm and room temperature is < 30 dB/km after exposure at a dose rate of 73 Rad/sec and a total accumulated dose of 1 MRad. At the same accumulated dose but ~34X lower dose rate, induced attenuation of R1310-HTA fiber is predicted to be ~30 dB/km (using Eq. 2 and data in Fig. 1). Again, it is assumed that data can be extrapolated from 50 kRad to 1 MRad .

3.2 Gamma Radiation Testing of MM Fibers

Nufern manufactures both standard and "radiation tolerant" versions of MM fibers having graded-index profiles. The radiation tolerant versions tested in this study included the 50/125, 62.5/125 and the 100/140 type. All the three MM fibers are designed for short-reach interconnects to be used in the aerospace arena. The bandwidths of these fibers at the two wavelengths of interest are presented in Table 5.

Radiation induced attenuation versus total accumulated dose data for the three fibers at 850 nm and 1300 nm wavelengths are shown in Fig. 2 and Fig. 3, respectively. Up to a total dose of < 50 kRad, all three fibers exhibit

Table 4. SMF28® radiation data comparison.

Source	Rad/min	kRad	T(°C)	dB/km
Nufern	127.8	50	23	6.55
Reference 11	0.1	100	25	2.96
Reference 11	0.01	100	25	2.10
Reference 11	*127.8*	*50*	*25*	*4.77*

Table 5. Bandwidths of the MM fibers.

Wavelength (nm)	Bandwidth (MHz-km)		
	50/125	62.5/125	100/140
850	≥1000	≥160	≥200
1300	≥300	≥500	≥200

induced attenuation that increases with increasing accumulated dose. At 850 nm, increase is linear ($A = mD$, where m is the slope of the A versus D plot) whereas at 1300 nm, increase follows the power law model (Eq. 2). Best fit parameters of all the three MM fibers at the two wavelengths are listed in the respective figures. The MM fibers exhibit higher radiation induced attenuation, particularly at the lower wavelength. Fortunately, these MM fibers, which need to be radiation hardened, are used as relatively short links. At 850 nm and up to 40 kRad, these fibers are far from

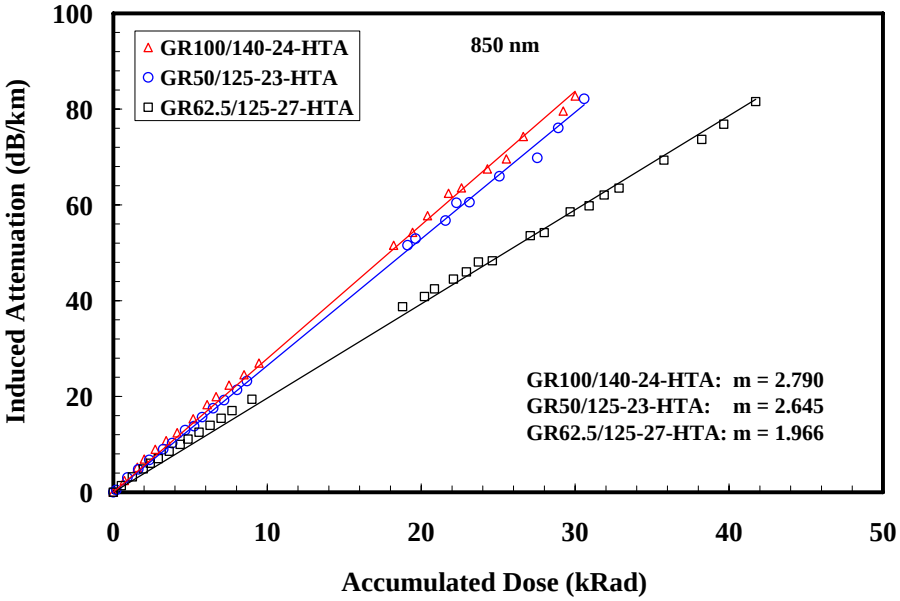

Fig. 2. γ-radiation data of the multimode fibers at 850 nm.

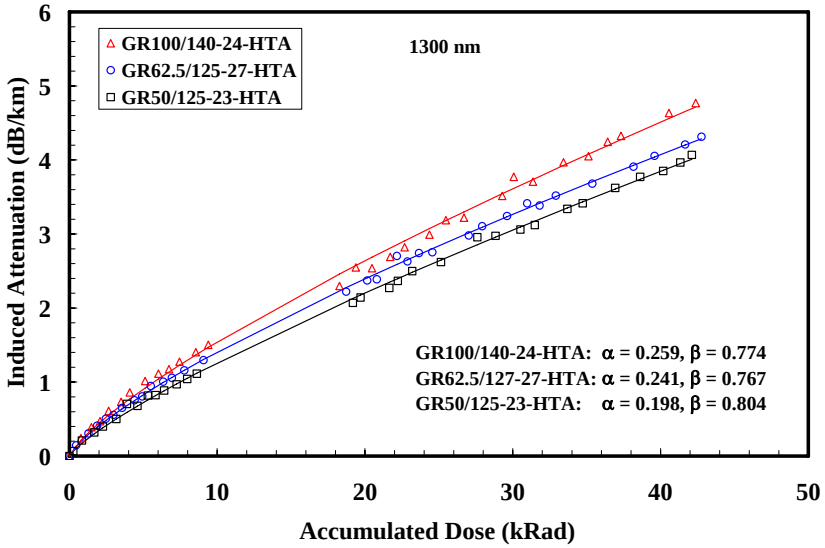

Fig. 3. γ-radiation data of the multimode fibers at 1300 nm.

Table 6. Multimode fibers radiation data comparisons.

Fiber Type	Designation/Manufacturer	Rad/sec	kRad	dB/m @ 1300 nm
62.5/125	BF04431® / OFS	0.54	46.8	581
62.5/125	BF04431® / OFS	0.083	37.1	498
62.5/125	*BF04431® / OFS*	*2.16*	*50*	*583*
62.6/125	GR62.5/125-25-HTA / Nufern	2.16	50	4.84
100/140	BF05444® / OFS	0.83	100	9.6
100/140	BF05444® / OFS	0.567	100	6.45
100/140	*BF05444® / OFS*	*2.16*	*50*	*21*
100/140	GR100/140-24-HTA / Nufern	2.16	50	5.35

reaching saturation. Similarly, at 1300 nm and up to 40 kRad, the fibers show no signs of saturation. In reference 11, gamma radiation hardness data is compiled for different types of MM fibers from various vendors at room temperature and at the two wavelengths. Again, comparison becomes difficult because of the widely different irradiation conditions. However, data is given for two of the OFS fibers (BF04431® and BF05444®) at two different dose rates that allow estimation of the induced loss under the conditions used in this study. Actual data is reproduced in Table 6 (in regular style) along with the values estimated using Eq. 3 (in italics). Nufern data is also presented. At 1300 nm, both the Nufern fibers exhibit superior radiation hardness than the competing fibers. One of the OFS fibers (BF04431®) does not appear to be of the radiation tolerant design.

3.3 Gamma Radiation Testing of PM Fibers

The PM fibers designated as PM1550G-80 and PM850G-80 are Panda style, 80 µm diameter, gyroscope-grade quality fibers that are designed to wind coils for high precision interferometric fiber optic gyroscopes (IFOGs) operating at 1550 nm and 830 nm, respectively. Induced attenuation versus accumulated dose plots of the two fibers are presented in Fig. 4. Once again, data for PM1550G-80 fiber (at 1550 nm) can be represented well by the "power law" model while data for PM850G-80 (at 830 nm) follows the linear model. Best fit parameters of both the PM fibers at the two wavelengths are listed in Fig. 4. Some information is available in the literature on the performances of PM fibers in γ-radiation environments. Reference 11 provides such data for a number of PM fibers. The data is reproduced in Table 7 along with the data for Nufern fibers. The two 3M fibers are of the elliptical cladding design for operation at 1550 nm (FS-PM-7621®) and at 820 nm (FS-PM4611®). FS-PM-7621® is an 80 µm size fiber while FS-PM-4611® is a 125 µm

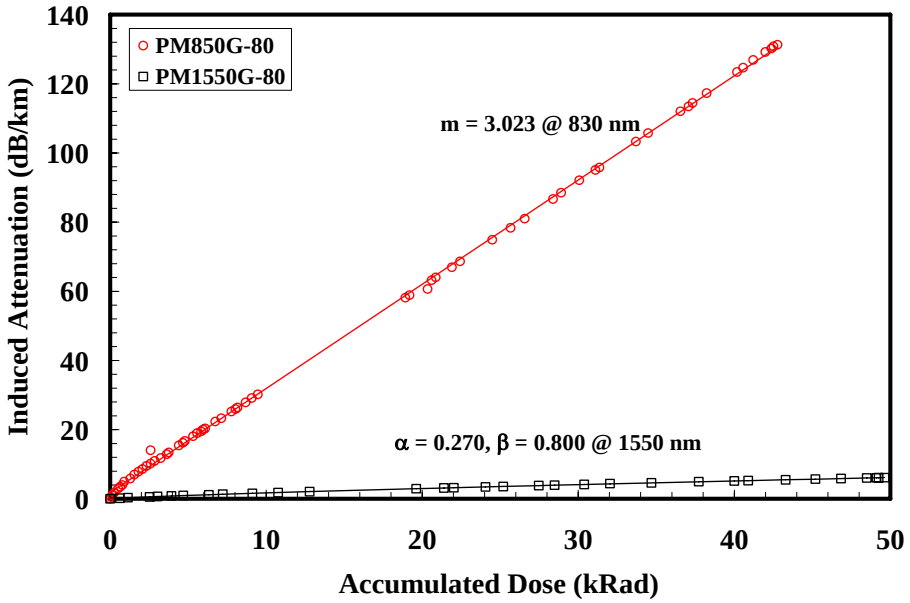

Fig. 4. γ-radiation data of the polarization maintaining fibers at the wavelengths of interest.

Table 7. Polarization maintaining fiber radiation data comparisons.

Fiber	Manufacturer	Rad/sec	kRad	dB/m
PM1550G-80	Nufern	2.1	50	6.2
FS-PM-7621®	3M	175	500	20
FS-PM-7621®	3M	175	5000	55
PM850G-80	Nufern	2.1	50	151
FS-PM4611®	3M	0.2	17	47
FS-PM4611®	3M	0.2	200	170
HB800®	Fibercore	21.2	10	45.6

size fiber. Both are considered as gyro-grade quality fibers. The comparison is made difficult by the widely different irradiation conditions. The Fibercore product (HB800®) is of the bow-type design and is an 80 μm diameter gyro-fiber for operation at 850 nm. Although one-on-one comparison is difficult because of the widely different irradiation conditions, photobleaching effects were present in the Fibercore fiber,[11] perhaps yielding an artificially lower induced attenuation.

3.4 Proton Radiation Testing

The near-earth space in which the satellites operate is dominated by energetic protons. However, radiation tolerance measurements are usually performed using γ-radiation because of the ready availability of such facilities. Another reason for the use of γ-radiation is the assumption that it provides a worse case scenario as compared to proton exposure. Past studies with proton irradiation have indeed determined that pure silica core and some doped fibers perform similarly or even better in comparison with exposure to γ-radiation. The proton radiation sensitivity of Nufern S1550-HTA (PSC), PM300G-80 (Ge-doped core) and EDFL-980-HP fibers were measured. The EDFL-980-HP fiber is designed to operate in the L-band and has high erbium concentration. Corning's SMF28® and Sumitomo's Z-fiber® were also tested for reference purposes. Both growth and recovery data were collected.

3.4.1 Proton Radiation Induced Attenuation Growth

Induced attenuation growth versus accumulated proton dose plots for S1550-HTA and Z-fiber® are shown in Fig. 5. S1550-HTA fiber with the higher NA (0.16) performs fairly well in comparison to Z-fiber® which has relatively smaller NA (0.12). For both the fibers, attenuation growth data can be represented well by the three-term "saturating

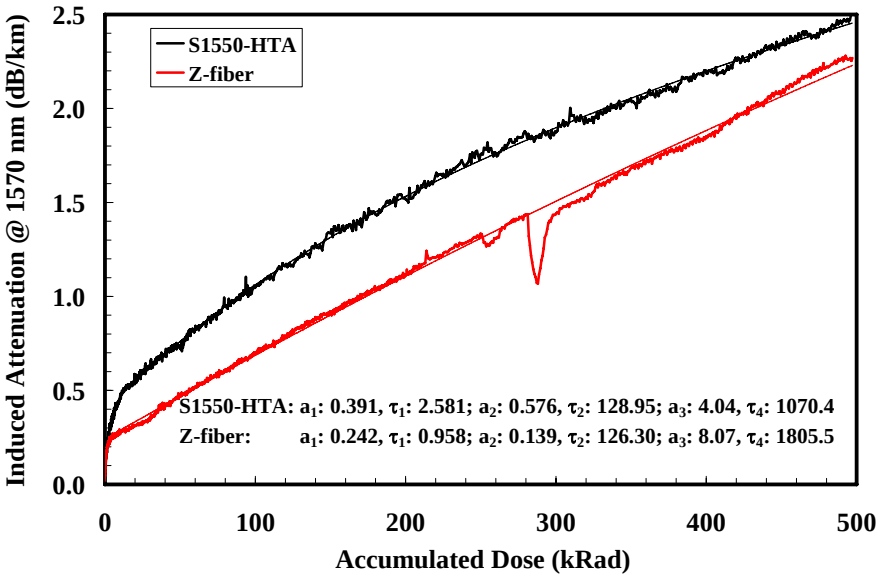

Fig.5. Proton radiation data of S1550-HTA and Z-fiber®.

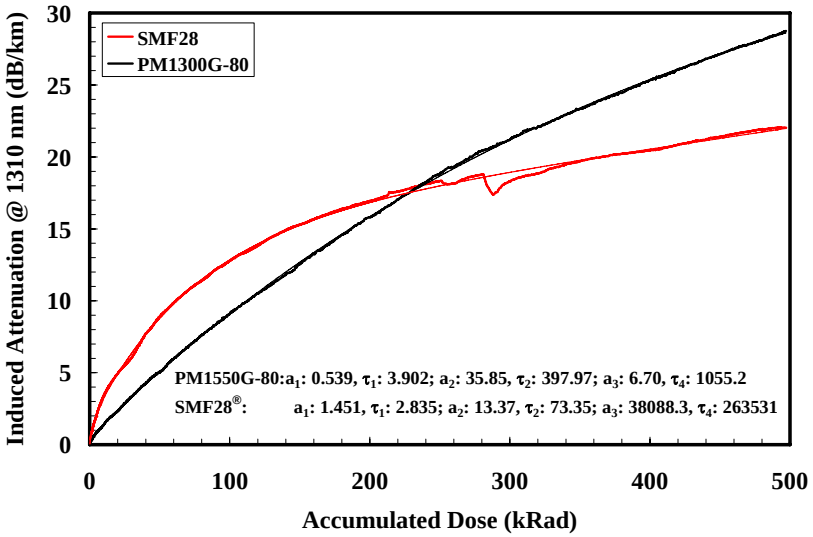

Fig. 6. Proton radiation data of PM1550G-80 and SMF28®.

exponentials" model described earlier (Eq. 1). Solid lines in Fig. 5 represent best fit to the data. The best fit parameters are also presented in Fig. 5. S1550-HTA shows a trend towards saturation while Z-fiber® does not indicate any such behavior. Using the data in Fig. 1 and Fig. 5, radiation induced-attenuation of S1550-HTA fiber at room temperature and to a total accumulated dose of 50 kRad is predicted to be 1.33 dB/km and 0.76 dB/km in γ- and proton radiation environments, respectively. The two induced attenuation versus total dose curves have different shapes (visually), a conclusion that is also supported by different fit parameters for each fiber. The shapes are governed by two competing factors: (i) color center formation and subsequent fiber darkening during irradiation, and (ii) recovery from thermal or photon induced annealing. Of course these processes are occurring at different rates in each fiber, suggesting that the origins of these defects in each fiber are different.

Induced attenuation growth versus accumulated proton dose plots for PM1300G-80 and SMF28® fibers are shown in Fig. 6. Both fibers have Ge-doped cores but different numerical apertures. For both the fibers, attenuation growth data can be represented well by the three-term "saturating exponentials" model described earlier (Eq. 1). Solid lines in Fig. 6 represent best fit to the data. The best fit parameters are also presented in Fig. 6. While attenuation of PM1300G-80 fiber increases continuously with increasing dose, attenuation of SMF28® rises rapidly at first and then reaches saturation at lower total dose. As in the previous case, the two induced attenuation versus total dose curves have different shapes suggesting that origins of defects in PM1300G-80 and SMF28® are different.

Most meaningful understanding of the performance of PM1300G-80 fiber can come from comparison with a similar fiber from another vendor. We were not able to find proton radiation data on any other PM fiber (gyro or non-gyro grade). However, comparison can be made with gamma radiation data. In reference 11 gamma radiation data is presented for 3M's PM1300 gyro fiber (FS-PM-6811®) which has an NA of 0.18 and contains a UV cured acrylate coating. Comparison is made in Table 8. Although measurement wavelength and temperature are roughly similar, higher numbers for the Nufern fiber should be viewed in light of and the fact that Nufern fiber was tested at a dose rate that was 165X larger.

Table 8. Polarization maintaining fiber proton radiation data comparison.

Manufacturer	λ (nm)	T (°C)	Rad/sec	kRad	dB/km
3M	1300	25	0.2	17	1.3
3M	1300	25	0.2	200	7.0
Nufern	1310	27	33	17	2.1
Nufern	1310	27	33	200	15.8

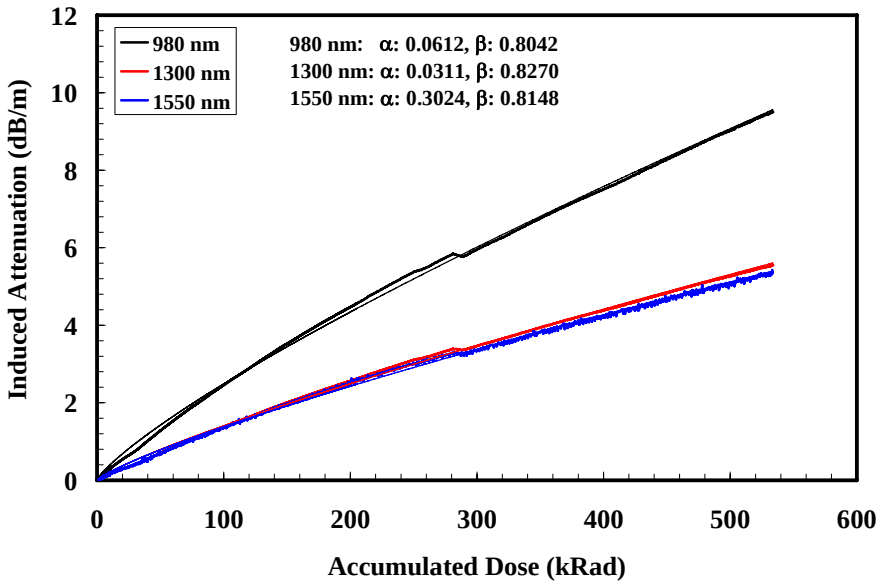

Fig. 7. Proton radiation data of Nufern EDFL-980-HP fiber at 980 nm, 1300nm and 1550 nm.

Induced attenuation growth (under passive conditions) versus accumulated proton dose plots of Nufern EDFL-980-HP fiber at the three wavelengths of interest are shown in Fig. 7. This fiber has Ge, Al and Er in the core. At each wavelength and up to 540 kRad, radiation induced attenuation growth versus accumulated dose data follows the power law model (Eq. 2). Solid lines in Fig. 7 represent best fit to the data. The best fit parameters are also presented in Fig. 7. Rose et. al.[14] studied the proton radiation induced attenuation of several Er-doped fibers manufactured by Lucent (later Spectran Corp. and now OFS). Protons had energies of 5.6 MeV and 28 MeV, and the fibers received a total dose of 50 kRad at a dose rate of 14 Rad/sec. Their data (after extrapolation from figures) is presented in Table 9 along with the data for Nufern fiber at the same total dose. Obviously radiation performance depends on the fiber composition. In addition, Nufern fiber was tested at twice the dose rate. The measurement temperature of Lucent fibers is also not known.

3.4.2 Recovery of the Proton Radiation Induced Attenuation

Actual dose rates in space radiation environments are fairly low, and measuring the optical fiber attenuations at such low dose rates with significant amounts of accumulated doses requires data collection over long periods of time that are impractical. However, it is possible to predict attenuations at low dose rates with significant amounts of accumulated doses using attenuation growth data obtained from short term but high dose rate experiments followed by measurements of attenuation recovery over time.[15] In general, prediction of attenuation after low dose rate exposures over prolonged time period involves: (i) exposure of fiber to lifetime dose, $D(t_f)$, at high dose rate, (ii) measurement of attenuation recovery and fit to x^{th} order kinetic model, and (iii) extrapolation by calculating incremental loss for $t = t_f$.

After the proton beam was shut-off, transmissions in all the fibers were monitored continuously for several hours to collect the recovery data. Recovery data was fitted to the following empirical model describing the x^{th} order kinetics:[15]

Table 9. Er-doped fiber proton radiation data comparison.

Manufacturer	Fiber	Rad/sec	kRad	Induced Attenuation (dB/m)		
				980 nm	1300 nm	1550 nm
Lucent	HP980	14	50	~3.1	~0.9	~0.5
Lucent	HE980	14	50	~0.5	~0.25	~0.15
Nufern	EDFL-980-HP	33	50	~1.4	~0.8	~0.7

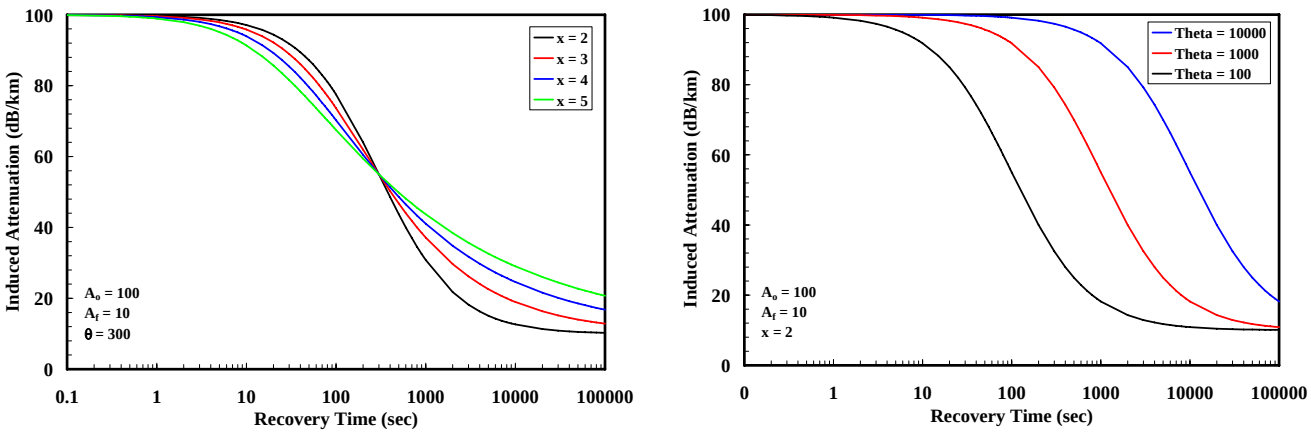

Fig. 8. Effects of parameters x and θ (in Eq. 4) on the shapes of the recovery plots.

$$A(t) = A_f + (A_o - A_f)/[1+(2^{x-1}-1)(t/\theta)]^{1/x-1} \quad (4)$$

where $A(t)$ is the induced attenuation at time t (sec), A_o is the induced attenuation (dB/length) at the beginning of recovery, A_f is the induced attenuation (dB/length) at the end of recovery, x is the kinetic order, and θ is the half life of the induced attenuation. Half life represents the time it takes for induced attenuation to decrease from A_o to $(A_o - A_f)/2$. A one, two or even higher term kinetic equation may be used to fit the recovery data. Shape of the recovery plot is highly dependent on parameters x and θ. Hypothetical plots of Eq. 4 indicating the effect of x and θ on the shape are presented in Fig. 8. Small x and θ give short and rapid decay, while large x and θ give long and slow decay.

Radiation induced attenuation recovery versus time plots for the S1550-HTA and the Z-fiber® are presented in Fig. 9 along with the fitted data. S1550-HTA fiber recovers faster and to a greater extent than the Z-fiber®. A two-term x^{th} order kinetic model fitted the data well for the Z-fiber® but the fit was not as good for the S1550-HTA fiber (may require 3 or 4 term model). For the S1550-HTA fiber, first recovery data was taken ~20 seconds after the end of the proton irradiation during which the induced attenuation recovered from 2.53 dB/km to 2.35 dB/km. Although under

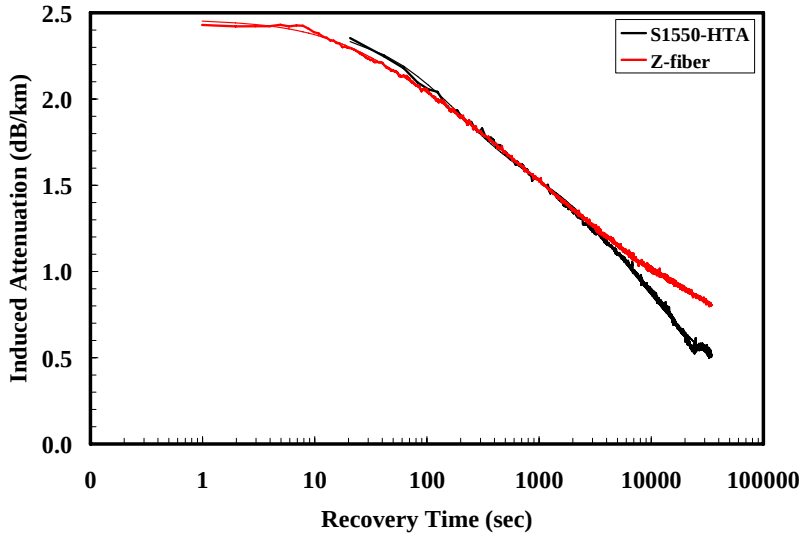

Fig. 9. Recovery plots of S1550-HTA and Z-fiber®.

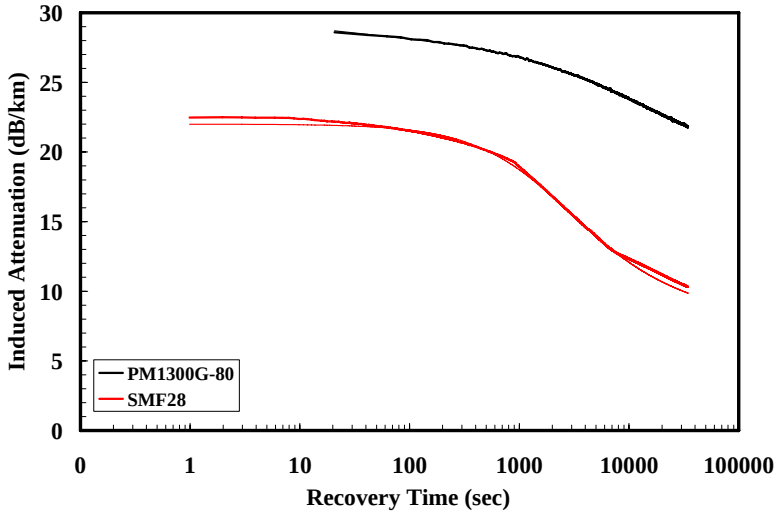

Fig. 10. Recovery plots of PM1300G-80 and SMF28®.

similar total proton dose of up to 500 kRad, S1550-HTA fiber exhibits higher attenuation than Z-fiber®, if both fibers started to recover at the same time, about 2500 sec later, S1550-HTA fiber will exhibit lower induced attenuation than Z-fiber® due to its faster recovery rate.

Radiation induced attenuation recovery versus time plots for the PM1300G-80 and SMF28® fibers are presented in Fig. 10 along with the fitted data. Again a two term x^{th} order kinetic model fitted the data very well for PM1300G-80 but the fit was not as good for the SMF28® and the fit may require 3 or 4 terms. As before, the first recovery point for PM1300G-80 was taken ~20 sec after the proton beam was shut-off and during this time the fiber recovered from a value of 28.8 dB/km to 28.6 dB/km. When exposed to a total dose of ~500 kRad, PM1300G-80 fiber attains higher attenuation relative to SMF28® and the recovery of attenuation after the end of irradiation is also slower relative to SMF28®. Radiation induced attenuation recovery versus time plots for the EDFL-980-HP fiber are presented in Fig. 11 along with the fitted data. The recovery is slow at all the three wavelengths. Agreement between experimental data and the 2-term x^{th} order kinetics is excellent.

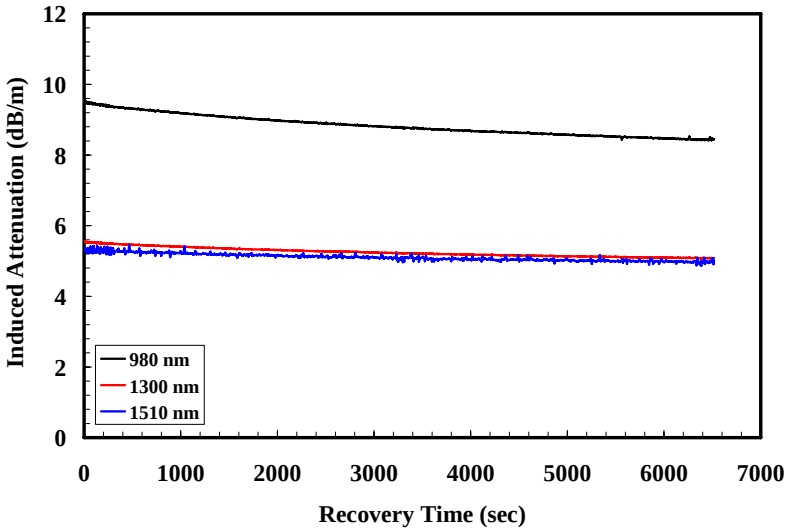

Fig. 11. Recovery plots of EDFL-980-HP fiber at three different wavelengths.

Table 10. High dose rate recovery parameters for various fibers.

Fiber	Term 1				Term 2			
	A_{o1} (dB/km)	A_{f1} (dB/km)	x_1	θ_1 (sec)	A_{o2} (dB/km)	A_{f2} (dB/km)	x_2	θ_2 (sec)
S1550-HTA	0.889	0.148	1.242	127.0	1.541	0.000	2.349	14106
Z-fiber®	0.445	0.090	1.483	34.79	2.007	0.000	5.757	6601
PM1300G-80	3.201	0.030	6.723	200.0	26.40	0.570	13.86	14400000
SMF28®	13.00	0.700	2.00	2799	9.000	2.300	9.000	5400000
EDFL 980 nm	0.251	0.017	13.52	200	9.338	0.496	11.13	3000000
EDFL 1300 nm	0.635	0.566	13.42	500	4.929	0.933	12.51	6500000
EDFL 1510 nm	0.636	0.688	13.94	500	4.659	1.481	13.01	8700000

High dose rate recovery parameters A_o, A_f, x and θ (for the two terms) for all the fibers tested for recovery after the termination of proton irradiation are presented in Table 10. At the beginning of recovery ($t_r = 0$), $A(0) = A_{o1}+A_{o2}$ while at the end of recovery ($t_r = \infty$), $A(\infty) = A_{f1}+A_{f2}$. $A(\infty)$ is a measure of the permanent damage. Among the Nufern fibers, S1550-HTA exhibits the lowest induced attenuation up to ~500 kRad and the smallest amount of permanent damage.

3.4.3 Predicting Radiation Induced Loss under Low Dose Rate Conditions

Predicting the radiation induced attenuation of fiber exposed to a slow dose rate up to the end-of-life time t_f from high dose rate experiments corresponding to time t_e is the key challenge. This estimation involves the following procedure:

(1) Knowledge of t_f and $D(t_f)$. As an example, if it is assumed that in a shielded location of a spacecraft interior, average radiation dose rate is 25 kRad/year over a 10 year lifetime of the spacecraft, then t_f = 10 years and $D(t_f)$ = 250 kRad.

(2) Knowledge of the fitted recovery parameters obtained by fitting the recovery data to x^{th} order kinetics following high dose rate exposure.

(3) Calculate the end-of-life attenuation $A(t_f)$ at t_f using the fitted recovery parameters and Eq. 4.

(4) $A(t_f)$ calculated in step-3 needs correction to account for the lower accumulated dose. Correction factor is calculated from high dose rate attenuation growth data as $A[D(t_f)]/A[D(t_e)]$.

(5) Calculate true attenuation $A(t_f)^* = A(t_f)$ x $A[D(t_f)]/A[D(t_e)]$.

Sample calculations are presented in Table 11. A very low attenuation is predicted for S1550-HTA fiber. As the end-of-life dose decreases, fibers will perform even better in the LEO spacecraft environment. The prediction accuracy will improve with recovery data collection over longer time periods.

4. CONCLUSIONS

Experimental data on γ- and proton-radiation hardness/tolerance of several of the Nufern fibers that include SM, MM,

Table 11. Attenuations in the fibers at the end-of-life.

Fiber	$D(t_e)$ (kRad)	$A(t_e)$ (dB/km)	$A(t_f)$ (dB/km)	Correction Factor	$A(t_f)^*$ (dB/km)
S1550-HTA	497.1	2.430	0.148	0.703	0.104
Z-fiber®	497.3	2.452	0.194	0.588	0.114
PM1300G-80	497.1	29.60	10.889	0.652	7.100
SMF28®	497.3	21.00	5.016	0.818	4.103
EDFL-980-HP (980 nm)	533.2	9.589	2.975	0.544	1.618
EDFL-980-HP (1310 nm)	533.2	5.564	1.895	0.534	1.013
EDFL-980-HP (1550 nm)	533.2	5.295	1.887	0.540	1.019

PM and erbium doped fiber versions which find application in earth orbiting satellites have been presented. It is hoped that this information will alleviate some of the concerns regarding paucity of such valuable data that is so desperately needed by the designers of satellites and their payloads. Nufern is undertaking this activity on a continuous basis and more data would be forth coming in future.

ACKNOWLEDGEMENTS

The authors would like to thank Dr. E. J. Friebele of the NRL, USA for conducting proton irradiation measurements.

REFERENCES

1. www.inetdaemon.com

2. J. A. Van Allen and L. A. Frank, L, "Radiation Around the Earth to a Total Distance of 107,400 km", *Nature*, 183, 430 (1959)

3. M. N. Ott, et. al., "Space Flight Requirements for Fiber Optic Components – Qualification Testing and Lessons Learned", *Proc. SPIE*, Vol. 6193 (2006). (To be published)

4. M. N. Ott, "Radiation Effects Expected for Fiber Laser/Amplifier Rare Earth Doped Optical Fiber", Survey Report, Sigma Research and Engineering, NASA GSFC, Parts Packaging and Assembly Technologies Office, March 2004

5. K. Arai, H. Imai, J. Isoya, H. Hosono, Y. Abe and H. Imagawa, "Evidence of Pair Generation of an E' Center and a Nonbridging Oxygen-Hole Center in γ-Ray Irradiated Fluorine Doped Low OH Synthetic Silica Glasses", *Phys. Rev. B*, 45(18), 10818-10821 (1992)

6. http://www.nufern.com

7. http://www.corning.com

8. http://www.sumitomoelectricusa.com

9. Y. Morita and W. Kawakami, "Dose Rate Effects on Radiation Induced Attenuation of Pure Silica Core Optical Fibers", *IEE Trans. Nucl. Sci*., 36, 584-590 (1989)

10. D. L. Griscom, M. Gingerich and E. J. Friebele, "Radiation Induced Defects in Glasses: Origin of Power Law Dependence of Concentration of Dose", *Phys. Rev. Lett.*, 71, 1019-1022 (1993)

11. M. N. Ott, "Radiation Effects Data on Commercially Available Optical Fiber - Database Summary", *Data Workshop Proceedings*, Nuclear Science & Radiation Effects Conference, Phoenix, AZ, 2002

12. E. J. Friebele, M. E. Gingerich and D. L. Griscom, "Extrapolating Radiation Induced Loss Measurements in Optical Fibers from the Laboratory to Real World Environments", *4th Biennial DoD Fiber Optics & Photonics Conference*, McLean, VA, 87-90, March 22-24, 1994

13. http://www.j-fiber.com

14. T. S. Rose, "Gamma and Proton Radiation Effects in Erbium-Doped Fiber Amplifiers: Active and Passive Measurements", *J. Lightwave Technol*., 19(12), 1918-1923 (2001)

15. E. J. Friebele, L. A. Brambani, M. E. Gingerich, S. J. Hickey and J. R. Onstott, "Radiation Induced Attenuation in Polarizing Maintaining Fibers: Low Dose Rate Response, Stress and Materials Effects", *Applied Optics*, 28(23), 5138-5143, 1989

In Proc. SPIE, vol. 6308, SPIE Optics and Photonics Conference on Photonics for Space Environment XI, Photonics Technology for Radiation Environment, August 14-18, 2006